Healing of Retinal Photocoagulation Lesions

Yannis M. Paulus, ATul Jain, Ray F. Gariano, Boris V. Stanzel, Michael Marmor, Mark S. Blumenkranz, and Daniel Palanker

Purpose. To systematically assess the changes in retinal morphology during the healing of retinal photocoagulation lesions of various clinical grades.

Methods. Rabbits were irradiated with a 532-nm Nd:YAG laser with a beam diameter of 330 μm at the retinal surface, a power of 175 mW, and pulse durations between 5 and 100 ms. Retinal lesions were clinically graded 1 minute after placement as invisible, barely visible, light, moderate, intense, very intense, and rupture and were assessed histologically at six time points from 1 hour to 4 months.

Results. At all pulse durations, the width of the retinal lesions decreased over time. At clinical grades of light and more severe (pulse durations, 10–100 ms), retinal scarring stabilized at 1 month at approximately 35% of the initial lesion diameter. Lesions clinically categorized as barely visible and invisible (pulse durations of 7 and 5 ms) exhibited coagulation of the photoreceptor layer but did not result in permanent scarring. In these lesions, photoreceptors completely filled in the damaged areas by 4 months.

Conclusions. The decreasing width of the retinal damage zone suggests that photoreceptors migrating from unaffected areas fill in the gap in the photoreceptor layer. Laser photocoagulation parameters can be specified to avoid not only the inner retinal damage, but also permanent disorganization and scarring in the photoreceptor layer. These data may facilitate studies to determine those aspects of laser treatment necessary for beneficial clinical response and those that result in extraneous retinal damage. (*Invest Ophthalmol Vis Sci.* 2008;49:5540–5545) DOI:10.1167/iovs.08-1928

Retinal laser photocoagulation was first described 45 years ago[1] and remains the standard of care for many retinal diseases. Panretinal photocoagulation (PRP) for proliferative diabetic retinopathy involves the purposeful destruction of a significant fraction of the photoreceptors, as well as other more superficial retinal layers.[2] Several mechanisms have been suggested to underlie the efficacy of PRP and other laser treatments, including improved retinal oxygenation, reduction in metabolic activity, inhibition of angiogenic stimulators, increased production of angioinhibitory factors, and oxidative stress.[3–6] Side effects of PRP treatment include permanent retinal scarring, resulting in scotomas and decreased peripheral, color, and night vision.[7] It remains largely unknown how these putative benefits of PRP or its many deleterious side effects[7] relate to parameters of laser treatment and subsequent retinal healing. Several investigators have presented evidence that light PRP (minimum-intensity photocoagulation)[8,9] or even subvisible treatment (micropulse photocoagulation)[10,11] has an efficacy equivalent to that of conventional PRP in causing regression of high-risk proliferative diabetic retinopathy and is associated with fewer complications and fewer treatment sessions. In a recent report, at 12 months, light PRP was equivalent to classic PRP in reduction or elimination of diabetic macular edema, visual improvement, change in contrast sensitivity, and decreased foveal retinal thickness on OCT.[8] Both of these approaches claim to offer the therapeutic benefit of conventional therapy without many of its side effects.[12] However, many physicians remain skeptical about these claims, and a prospective randomized clinical trial is needed to provide convincing evidence one way or the other.

Recent studies have begun to explore the evolution of laser-induced retinal lesions over time.[13] Retinal lesions in rats were shown to stabilize by 60 days.[14] Immunohistochemical studies of the laser lesions in mice 4 weeks after treatment have shown that the healing processes are driven by cells and vessels that are retinal in origin.[14,15] It has also been found that the lesion size in rodents decreases over time due to migration of photoreceptors from the untreated surrounding areas, filling in the damaged outer retina.[16] Healthy adjacent photoreceptors have been shown to repopulate regions of photoreceptor damage in a process associated with actin.[17] The lesions of 200 μm showed resolution of damage in the photoreceptor layer, whereas 800-μm lesions did not.[16] This observation suggests that photoreceptor migration may have a finite limit.[16] Postinjury proliferation and migration of neurons have also been recently described in several other neuronal systems.[18–21] Although rodent studies have provided important insight into the dynamics of retinal healing and remodeling, the lack of retinal scarring in rodents makes it a suboptimal model for retinal photocoagulation lesions in humans.

In this study we provide a systematic histologic analysis of the effects of retinal photocoagulation and describe the dynamics of healing and reorganization of retinal lesions of various clinical grades in rabbits. This study of laser-induced retinal lesions was facilitated by the use of a recently developed semiautomated retinal photocoagulation system (PASCAL; OptiMedica Inc., Santa Clara, CA).[22] This delivery system allows for creating well-aligned arrays of retinal lesions with variable durations of laser exposure and power. The effects of pulse duration and laser power on the initial size and character of retinal photocoagulation lesions in rabbits have been described.[22,23] The purpose of the present study was to determine the treatment parameters for retinal photocoagulation that allow avoiding not only inner retinal damage, but also permanent disorganization and scarring in the photoreceptor layer. This study is a step toward determination of those aspects of laser treatment necessary for clinical response and those that result in extraneous retinal damage.

From the Department of Ophthalmology, Stanford University School of Medicine, Stanford, California.

Supported by an Alcon Research Institute grant, the Horngren and Miller Family Foundations, OptiMedica Corp., the Angelos and Penelope Dellaporta Research Fund, and the L. Boltzmann Institute for Retinology and Biomicroscopic Laser Surgery, Vienna, Austria.

Submitted for publication February 24, 2008; revised June 29, 2008; accepted September 26, 2008.

Disclosure: **Y.M. Paulus**, None; **A. Jain**, None; **R.F. Gariano**, None; **B.V. Stanzel**, None; **M. Marmor**, None; **M.S. Blumenkranz**, OptiMedica Corp. (I, C, P); **D. Palanker**, OptiMedica Corp. (I, C, P)

The publication costs of this article were defrayed in part by page charge payment. This article must therefore be marked "*advertisement*" in accordance with 18 U.S.C. §1734 solely to indicate this fact.

Corresponding author: Daniel Palanker, Stanford University Department of Ophthalmology, 300 Pasteur Drive, Room A157, Stanford, CA 94305-5308; palanker@stanford.edu.

METHODS

Pattern Scanning Photocoagulation

This laser system (PASCAL; OptiMedica Inc.) provides 532 nm optical radiation from a diode-pumped, continuous wave, frequency-doubled Nd:YAG laser coupled to a multimode step index optical fiber. The exit surface of the fiber is telecentrically imaged through the scanning system onto the retina with variable magnification, thus providing a variety of spot sizes with nominally top-hat intensity profiles. At the aerial image plane of the slit lamp microscope the laser spots measure 500 μm in diameter, with the laser intensity transition from 10% to 90% occurring over 6 μm. Variation of the beam intensity within the top-hat area does not exceed $\pm$7%. A touch-screen graphic user interface is used to control laser parameters including the spot size, laser power, pulse duration, and pattern geometry. Once the treatment parameters are appropriately selected, a foot pedal is used to activate the laser.

Retinal Laser Application

Eighteen Dutch Belted rabbits (weight, 2–3 kg) were used in accordance with the ARVO Statement for the Use of Animals in Ophthalmic and Vision Research, after approval from the Stanford University Animal Institutional Review Board. The rabbits were anesthetized with ketamine hydrochloride (35 mg/kg, IM), xylazine (5 mg/kg, IM), and glycopyrrolate (0.01 mg/kg, IM), administered 15 minutes before the procedure. Pupillary dilation was achieved by 1 drop each of 1% tropicamide and 2.5% phenylephrine hydrochloride. Topical tetracaine 0.5% was instilled in the treated eye before treatment. Only one eye of each rabbit was treated, unless the rabbit was to be killed immediately.

A standard retinal laser contact lens (Mainster model OMRA-S; Ocular Instruments, Bellevue, WA) was used to focus the laser on the rabbit fundus. Taking into account the combined magnifications of the contact lens and rabbit eye of 0.66,[24] the aerial image of 500 μm corresponded to a retinal spot size of 330 μm. Using modified scanning software, columns consisting of six exposures with pulse durations of 5, 7, 10, 15, 20, 50, and 100 ms were applied. Five identical columns were applied in each eye to broaden the statistical base of the study. Laser power was maintained at 175 mW for all lesions. Placement of larger marker burns adjacent to the patterned lesions facilitated later histologic localization of the barely visible and invisible lesions.

The clinical appearance of the laser lesions were graded by a single masked observer within 1 minute after the treatment according to the following scale: invisible, barely visible, light, moderate, intense, very intense, and rupture. The barely visible lesions were defined as a faint lightening of the fundus pigmentation. Light burns exhibited further blanching but without frank whitening. Moderate lesions exhibited definite retinal whitening without adjacent edema, and intense burns displayed central whitening and a halo of translucent edema. Very intense lesions had a more marked and complete central retinal whitening and a larger ring of edema. A rupture was assumed to have occurred if small bubbles with or without hemorrhage appeared at the lesion site.

Retinal Histology

Rabbits (three in each group) were killed 1 hour, 1 day, 1 week, 1 month, 2 months, or 4 months after treatment with a lethal dose of an IV barbiturate (Beuthanasia; Schering-Plough Animal Health Corp., Kenilworth, NJ) in an ear vein. The eyes were enucleated and fixed in 1.25% glutaraldehyde/1% paraformaldehyde in cacodylate buffer at pH 7.2 overnight at room temperature. The eyes were then postfixed in osmium tetroxide, dehydrated with a graded series of ethanol, processed with propylene oxide, embedded in an epoxy resin, and sectioned into 1 μm-thick sections. Samples were stained with toluidine blue and examined by light microscopy.[25]

Serial sections of the retina were examined, and four burns from two different animals were analyzed for each of the six time points and seven pulse durations (168 in total). By visually scanning the serial sections, three widest lesions corresponding to each burn were measured using a microscope measuring scale. The lesion size was measured as the furthest extent of damage at the RPE-photoreceptor junction. These three measurements for each of the four burns were averaged, and representative lesions for each time point were photographed. The mean and SD of these 12 numbers were calculated (Excel; Microsoft, Redmond, WA). The total size of the measurements database was 504 numbers (168 $\times$ 3).

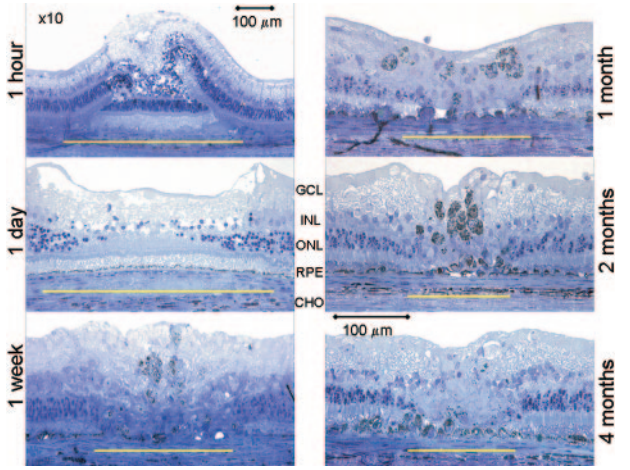

FIGURE 1. Figures 1 through 5 show progression of the lesions produced with a retinal beam size of 330 μm in diameter, with laser power of 175 mW. Sections were stained with toluidine blue. Photographs were taken via 20$\times$ microscope objective, except for a 1-hour lesion, which was photographed using 10$\times$ magnification due to its large size (and has its own scale bar). *Yellow bar*: the extent of damage at the RPE-photoreceptor junction. GCL, ganglion cell layer; INL, inner nuclear layer; ONL, outer nuclear layer; RPE, retinal pigment epithelium; CHO, choroid. Shown in this figure is a representative intense lesion produced by 100-ms pulse. The lesion encompassed all retinal layers. Pigmented cells invaded the full thickness of the retina from 1 week to 2 months. At 4 months, a scar occupied the 36% of the initial lesion.

Fluorescein Angiography

For fluorescein angiography (FA), 0.3 mL of contrast (Fluorescite 10%; (Alcon Laboratories, Hünenberg, Switzerland) was slowly (10 seconds) injected into the marginal ear vein as described elsewhere.[26] Fundus photographs were taken with a fundus camera (TRC 50$\times$ [Topcon, Tokyo, Japan], using a Kodak Megaplus Camera, Model 1.4 [Eastman Kodak, Rochester, NY], operated by Winstation imaging software [Ophthalmic Imaging Systems, Inc, Sacramento, CA]), starting a few seconds after the injection, and every 20 seconds for up to 5 minutes. Fluorescein angiography was performed 1 hour and 1, 3, and 7 days after the placement of lesions with all clinical grades: very intense, intense, moderate, light, barely visible, and invisible.

RESULTS

Histology

Intense Lesions. As shown in Figure 1, at 1 hour after treatment, intense lesions were sharply demarcated and encompassed all retinal layers, as well as the retinal pigment epithelium (RPE) and choroid. Retinal edema was present, and the normal laminar architecture of the retina was disorganized by displacement of the outer retina.

At 1 day, edema was nearly resolved in the inner and outer retina. The inner and outer nuclear layers (INL and ONL) were sparse and contained pyknotic nuclei. Photoreceptor inner segments appeared shortened, and the outer segments appeared in disarray. Even though RPE cells were clearly affected, the RPE pigmentation appeared largely normal. Hyaline (pale

TABLE 1. Relative Width of the Retinal Lesions of Various Grades over Time, as Measured at the RPE-Photoreceptor Junction

		Days after Treatment					
Clinical Grade	**Pulse Duration (ms)**	**0**	**1**	**7**	**30**	**60**	**120**
Intense	100	100	76	54	40	37	36
Moderate	50	100	91		42	39	37
Light-moderate	20	100	89	87	42	44	40
Light	15	100	92	82	35	38	38
Light	10	100	71	67	50	33	50
Barely visible	7	100	89	69	10	10	6
Invisible	5	100	72	34	15	1	0

Data are expressed as percentage of the initial lesion size. For each pulse duration, the width for all time points was normalized to the size of the retinal lesion at 1 hour. Intense to light lesions stabilized at approximately 40% of the initial lesion size at 2 months. Barely visible and invisible lesions continued to heal, so that there was no visible defect at the RPE–photoreceptor junction at 4 months.

blue) vacuoles were present between the basal RPE and Bruch's membrane. There appeared to be a loss of choroidal structures accompanied in part by vascular engorgement and exudation. The lateral extent of the damage zone became less clear because of scattered, enlarged INL and ONL cells at the lesion borders.

At 1 week, intense lesions had contracted to 54% of their initial diameter (Table 1). INL cells remain enlarged, but extracellular edema was now absent. Pigmented cells invaded the full thickness of the retina. Retinal architecture was now difficult to discern because of partial loss of cells and their replacement with gliotic tissue in all retinal layers. The RPE was discontinuous, with large pigmented clumps interspersed with depigmented areas. Multilayered hypopigmented cells were present on an intact Bruch's membrane. Vascular caliber had normalized in larger choroidal vessels, but remained decreased within the choriocapillaris, which was less dense. Choroidal thickness had returned to normal.

At 1 month, edema was absent and the lateral/horizontal width of the lesion was 40% of its initial size. Gliosis and pigmented cells are present in all retinal layers, and there was some central thinning. Hypertrophied and hyperpigmented RPE was present.

At 2 months, the lesions further contracted to 37% of the original lesion diameter, and otherwise appeared similar to lesions at 1 month.

At four months, the lesion diameter was still approximately 36% of the original lesion and similar in appearance as at 2 months, with the exception that intraretinal pigmented cells had disappeared and the lesion largely consisted of hypocellular matrix.

Light and Moderate Lesions. One hour after treatment the light-to-moderate lesion exhibits strong edema in the inner retina, damaged inner and outer nuclear layers, and large vacuoles in the inner segment layer (Figs. 2, 3). Choroidal changes are less pronounced than in the intense lesion.

At day 1, retinal edema had decreased considerably. Inner and outer segments of photoreceptors were strongly reduced, and nuclei in the ONL were small and pyknotic within the boundaries of the lesion. The INL nuclei appeared more round and enlarged, compared with the surrounding untreated retina. The central defect in ONL and INL of intense lesions was absent.

At 1 week, there was no significant choroidal involvement. ONL and most of the INL were replaced by gliotic tissue and were invaded by pigmented cells. Continuous hypopigmented RPE layer can be clearly seen in Figure 3.

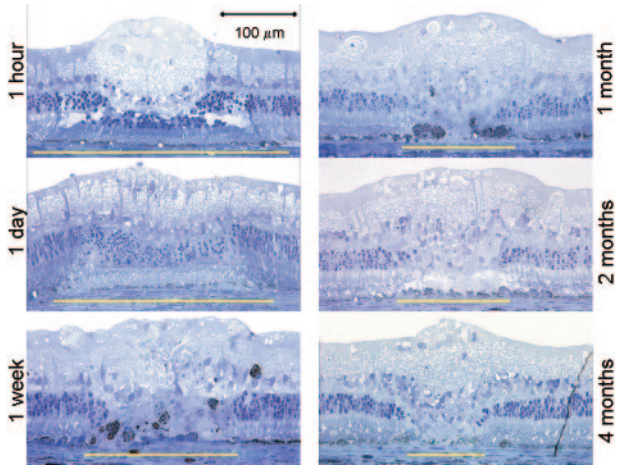

FIGURE 2. Light-moderate lesions (20-ms pulse duration) at initial stage (1 hour) involved strong edema in the inner retina above the destroyed layer of photoreceptors. Edema largely subsided by 1 day, and damaged photoreceptors were replaced with hypertrophied glia by 1 week. The scar was largely stabilized after 1 month and covered 40% of the initial lesion size at 4 months.

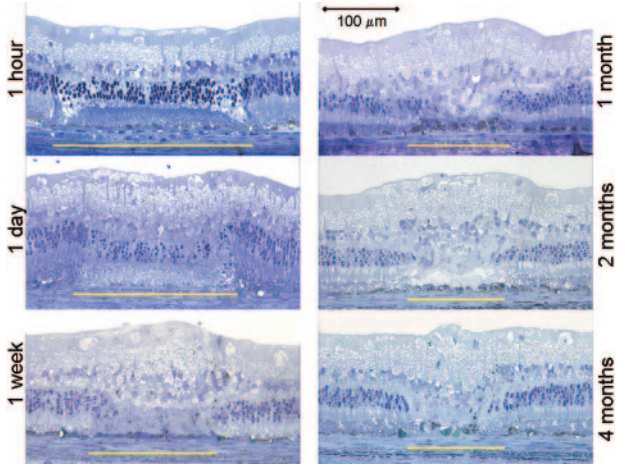

FIGURE 3. In the light lesions (15-ms pulse duration), initial damage was localized to the photoreceptors. The RPE layer was restored by 1 week, although the cells appeared hypopigmented. The width of the gliotic scar in the outer retina stabilized by 1 month at approximately 40% of its original size.

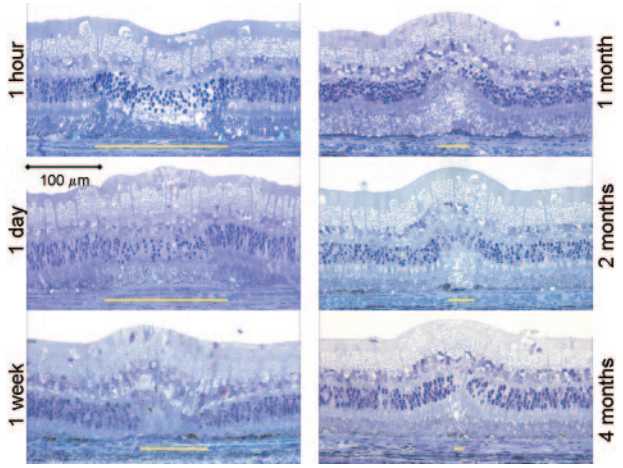

FIGURE 4. Barely visible lesions produced at 7-ms pulse duration exhibited perfect localization of the retinal damage to photoreceptors. Gliotic replacement of the damaged photoreceptors continued to contract over time, showing an outer retina with almost continuous normal morphology at 4 months.

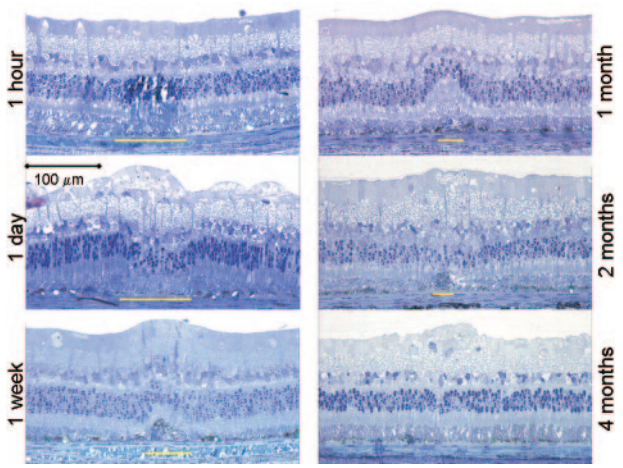

FIGURE 5. Invisible lesion produced with 5-ms pulse duration exhibited laser damage localized to photoreceptors and RPE. Damaged photoreceptors were replaced within a few weeks, with normal retinal morphology completely restored by 4 months.

At 1 month, the lesion had contracted asymmetrically and appeared larger toward the inner retina and smaller at the RPE. The INL was thickened, and its cells were enlarged in the center of the lesion. Photoreceptors filled the peripheral part of the lesion, leaving a remaining damage zone of 40% of the original width. The RPE was hyperpigmented in the lesion periphery with zones of hypopigmentation and pigmented cellular aggregates more centrally.

At 2 months, the cellular accumulation in the center of the lesion remained displaced toward the RPE, patchy gliosis filled in the cellular gaps in the photoreceptor layer, and a decreased number of hyperpigmented cells remained in the retina. RPE pigmentation appeared more continuous, with some small clumps of pigmented cells remaining. The width of the lesion continued to be 40% of its original size.

At 4 months, the lesion maintained its size at 40%, although the INL regained its normal structure at the periphery. The central portion of the INL remained displaced toward the RPE, and the gap in the photoreceptor layer remained filled in with gliosis and displaced INL cells.

Barely Visible and Invisible Lesions. As shown in Figure 4, the barely visible lesions differed both quantitatively and qualitatively from the more intense lesions. Initial lesion diameters were smaller than those of lesions created with longer pulse durations (see Fig. 6).

At 1 hour, the inner retina appeared largely unaffected, whereas the ONL was hyperchromatic. RPE seemed collapsed, but its pigmentation remained unchanged. Outer segments of photoreceptors were disorganized, and the nuclei were pyknotic.

At 1 day, there was slight edema in the inner retina, but both INL and GCL seemed to be only minimally affected. Inner segments of photoreceptors were shortened, the outer segments depigmented, and the ONL displaced toward the RPE. The RPE had a hypochromatic cytoplasm.

At 1 week, the INL was slightly expanded, and missing photoreceptors were probably replaced by glial elements. Retinal edema was mild and localized primarily to the outer retina. The RPE layer was restored, but seemed hypopigmented in the center of the lesion. The choroid appeared normal. The lesion contracted to 69% of its original size.

At 1 month, the lesion had contracted to 10% of its initial diameter. Histologic changes were localized to the outer retina and consisted of a thinned ONL and disorganized photoreceptors in the center of the lesion. Gliosis and downward displacement of the INL were notably absent. Intraretinal pigmented cells, present in more severe lesion grades, were absent as well.

At 2 months, the lesion was similar to that at 1 month. A few hyperpigmented RPE cells were evident only in the center of the lesion.

At 4 months, the lesion was distinguished from adjacent normal retina only by a few-cells-wide area of decreased density within the ONL with occasional adjacent vacuoles in the inner segments, and slight elevation. Mild and variable hyperpigmentation at the RPE level persisted in some lesions. Photoreceptor morphology within lesions was otherwise indistinguishable from that in untreated retina.

Histology of ophthalmoscopically invisible lesions (5-ms exposures) revealed even more localized damage to photoreceptors and RPE, with excellent preservation of the other retinal layers (Fig. 5). Healing of the lesion followed steps similar to those of the barely visible lesion, with even more

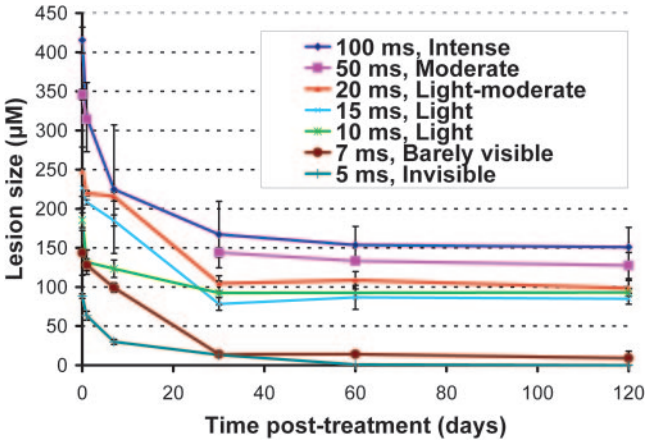

FIGURE 6. The width of the retinal lesions of various grades over time, as measured at the RPE–photoreceptor junction. All lesions decreased in size, and more intense lesions are wider initially. Moderate and intense burns stabilized at 150 μm and light to light-moderate burns stabilized at 100 μm by 2 months, with minimal change in size at 4 months. Barely visible and invisible lesions continued to heal to complete closure by 4 months. Error bars show the SD for each time point of each of four burns measured per time point.

complete resolution by the end of 4 months. In additional experiments, pulse durations of 3 ms and shorter failed to produce ophthalmoscopically visible burns. Retinal histology appeared entirely normal within the treated region (data not shown).

Changes in the lateral extent of the retinal lesions over time were summarized in the plot shown in Figure 6. Table 1 shows the relative lesion sizes over time, normalized on initial lesion size at 1 hour.

Fluorescein Angiography

At 1 hour and 1 day after laser application, all clinical grades of laser lesions (from invisible to very intense) exhibited hyperfluorescence with fluorescein angiography. At 3 days, light and more intense lesions remained hyperfluorescent, whereas clinically invisible and barely visible lesions were not evident on angiography. By 7 days after laser application, none of the lesions remained hyperfluorescent.

Discussion

The present study provides a systematic assessment of histologic changes over time in retinal photocoagulation lesions of various clinical grades in rabbits. Use of the pattern delivery system (PASCAL; OptiMedica Inc.) helped, with rapid and well-aligned application of multiple lesions with variable pulse durations. We achieved consistent clinical levels of lesion intensities by varying pulse duration while maintaining constant spot size and power settings. Since laser power, spot size, and pulse duration affect the resulting lesion character in a different fashion,[23] our results may not be entirely generalizable to lesions that differ in their clinical grade due to variations in spot size and/or power settings. Since lesion size decreases with decreasing pulse duration and laser power, more burns or larger laser spot sizes are necessary to treat an equivalent retinal area that may be essential to reach a similar clinical efficacy.

For all clinical grades, the lateral extent of retinal damage decreased over time, with the extent of reduction dependent on the initial width and the severity of the lesion. Within 2 months the intense, moderate, and light lesions decreased in width by a factor of 3, whereas the barely visible and invisible lesions disappeared nearly entirely. Retinal gliosis appeared only temporarily between 1 and 4 weeks in barely visible lesions, whereas in more intense burns, it stabilized by 1 month, and persisted at 4 months. The end-stage histology of the light, moderate, and intense burns is similar. Similar healing rates have been observed during experimental RPE debridement in rabbits.[27] Resolution of fluorescein angiography hyperfluorescence by 1 week corroborates the anatomic demonstration that RPE continuity was restored by 1 week (see for example, Fig. 3). For invisible and barely visible lesions, this continuity occurred even faster—by 3 days.

Lateral photoreceptor migration to replace initial cell loss has been suggested by previous studies in the rat retina.[16] However, restoration of the photoreceptor layer in rats was more rapid, reaching its maximum extent by 3 weeks, whereas we found this process continuing in rabbits throughout the 4-month period of observation, particularly in the first 2 months. In addition, retinal lesions in rats exhibit less gliosis than in rabbits. Observation of the photoreceptors migration in both the merangiotic rabbit model and the holangiotic rat model of retinal photocoagulation, indicate the likelihood of similar phenomenon in humans. High-resolution OCT imaging of the evolution of retinal lesions of various grades in patients could provide such evidence.

Photoreceptor outer segments damaged during selective RPE photocoagulation in rabbits have been shown to recover by 4 weeks after laser irradiation after initial disc disorganization and vacuolization.[28] However, it is unlikely that, in our case, photoreceptor restoration after retinal photocoagulation was due to the recovery of damaged outer segments since outer nuclear layer pyknosis at 1 day proceeded to large visible lesions devoid of nuclei at 1 week.

Remaining unknown is the role of neuronal regeneration in the restoration of the photoreceptor layer observed in our study, either through differentiation of resident neuronal stem cells at the ciliary margin[29–36] or the transdifferentiation of Müller glia.[37]

Regardless of the mechanism, restoration of retinal continuity has clinically important implications. If the therapeutic benefit of PRP involves reduction in the number of photoreceptors, it can be achieved more selectively using barely visible or invisible lesions without the permanent scarring of more intense lesions. Restoration of retinal continuity and absence of scarring might reduce microscotomas typical of conventional PRP and may also allow for retreatment.

In addition, such minimally traumatic therapy reduces the level of pain and discomfort associated with PRP. Application of the barely visible or invisible lesions is facilitated using arrays that can incorporate higher intensity visible marker burns at the corners (Pascal; OptiMedica Inc.). Such lesions enable proper placement of successive applications of arrays.

Our results may also form the basis for a useful model of retinal fibrosis. Fibrosis remains a major clinical problem in ophthalmology and is the key factor causing irreversible blindness in several diseases, including subretinal scarring in end-stage macular degeneration. We have shown that several features of retinal healing (e.g., cell death, edema, RPE invasion, gliosis, and matrix deposition) can be predictably isolated or combined within lesions by varying the parameters of laser treatment. Our descriptions of these graded responses may thus facilitate scientific investigation into discrete steps in retinal wound healing and allow for the assessment of potential therapies to prevent or resolve retinal fibrosis.

In summary, we have described the histopathology of retinal photocoagulation lesions across a wide spectrum of clinical grades and over an extended time course. These data may be useful in further evaluations of mechanisms of retinal healing and may form the basis for a rational approach to optimizing parameters for clinical retinal laser therapy.

Acknowledgments

The authors thank Roopa Dalal for histologic preparations and retinal lesion measurements; Philip Huie for help with animal housing and administration; and Dan Andersen, Georg Schuele, and Hiroyuki Nomoto for stimulating discussions.

References

1. Kapany NS, Peppers NA, Zweng HC, Flocks M. Retinal photocoagulation by lasers. *Nature.* 1963;199:146–149.
2. Little HL, Zweng HC, Peabody RR. Argon laser slit-lamp retinal photocoagulation. *Trans Am Acad Ophthalmol Otolaryngol.* 1970;74(1):85–97.
3. Jennings PE, MacEwen CJ, Fallon TJ, et al. Oxidative effects of laser photocoagulation. *Free Radic Biol Med.* 1991;11(3):327–330.
4. Sanchez MC, Luna JD, Barcelona PF, et al. Effect of retinal laser photocoagulation on the activity of metalloproteinases and the alpha(2)-macroglobulin proteolytic state in the vitreous of eyes with proliferative diabetic retinopathy. *Exp Eye Res.* 2007;85(5):644–650.
5. Spranger J, Hammes HP, Preissner KT, et al. Release of the angiogenesis inhibitor angiostatin in patients with proliferative diabetic retinopathy: association with retinal photocoagulation. *Diabetologia.* 2000;43(11):1404–1407.

6. Matsumoto M, Yoshimura N, Honda Y. Increased production of transforming growth factor-beta 2 from cultured human retinal pigment epithelial cells by photocoagulation. *Invest Ophthalmol Vis Sci.* 1994;35(13):4245–4252.
7. Fong DS, Girach A, Boney A. Visual side effects of successful scatter laser photocoagulation surgery for proliferative diabetic retinopathy: a literature review. *Retina.* 2007;27(7):816–824.
8. Bandello F, Polito A, Del Borrello M, et al. "Light" versus "classic" laser treatment for clinically significant diabetic macular oedema. *Br J Ophthalmol.* 2005;89(7):864–870.
9. Bandello F, Brancato R, Menchini U, et al. Light panretinal photocoagulation (LPRP) versus classic panretinal photocoagulation (CPRP) in proliferative diabetic retinopathy. *Semin Ophthalmol.* 2001;16(1):12–18.
10. Luttrull JK, Musch DC, Spink CA. Subthreshold diode micropulse panretinal photocoagulation for proliferative diabetic retinopathy. *Eye.* 2008;22(5):607–612.
11. Luttrull JK, Spink CJ. Serial optical coherence tomography of subthreshold diode laser micropulse photocoagulation for diabetic macular edema. *Ophthalmic Surg Lasers Imaging.* 2006;37(5):370–377.
12. Dorin G. Evolution of retinal laser therapy: minimum intensity photocoagulation (MIP): can the laser heal the retina without harming it? *Semin Ophthalmol.* 2004;19(1–2):62–68.
13. Marshall J, Hamilton AM, Bird AC. Histopathology of ruby and argon laser lesions in monkey and human retina: a comparative study. *Br J Ophthalmol.* 1975;59(11):610–630.
14. Ben-Shlomo G, Belokopytov M, Rosner M, et al. Functional deficits resulting from laser-induced damage in the rat retina. *Lasers Surg Med.* 2006;38(7):689–694.
15. Behar-Cohen F, Benezra D, Soubrane G, et al. Krypton laser photocoagulation induces retinal vascular remodeling rather than choroidal neovascularization. *Exp Eye Res.* 2006;83(2):263–275.
16. Busch EM, Gorgels TG, Van Norren D. Filling-in after focal loss of photoreceptors in rat retina. *Exp Eye Res.* 1999;68(4):485–492.
17. Zwick H, Edsall P, Stuck BE, et al. Laser Induced photoreceptor damage and recovery in the high numerical aperture eye of the garter snake. *Vision Res.* 2008;48(3):486–493.
18. Gould E, Gross CG. Neurogenesis in adult mammals: some progress and problems. *J Neurosci.* 2002;22(3):619–623.
19. Temple S. Stem cell plasticity: building the brain of our dreams. *Nat Rev Neurosci.* 2001;2(7):513–520.
20. Magavi SS, Leavitt BR, Macklis JD. Induction of neurogenesis in the neocortex of adult mice. *Nature.* 2000;405(6789):951–955.
21. Nakatomi H, Kuriu T, Okabe S, et al. Regeneration of hippocampal pyramidal neurons after ischemic brain injury by recruitment of endogenous neural progenitors. *Cell.* 2002;110(4):429–441.
22. Blumenkranz MS, Yellachich D, Andersen DE, et al. Semiautomated patterned scanning laser for retinal photocoagulation. *Retina.* 2006;26(3):370–376.
23. Jain A, Blumenkranz MS, Paulus Y, et al. Effect of pulse duration on size and character of the lesion in retinal photocoagulation. *Arch Ophthalmol.* 2008;126(1):78–85.
24. Birngruber R. Choroidal circulation and heat convections at the fundus of the eye. In: Wolbarsht ML, ed. *Laser Applications to Medicine and Biology.* New York: Plenum Press; 1991.
25. Turner KW. Hematoxylin toluidine blue-phloxinate staining of glycol methacrylate sections of retina and other tissues. *Stain Technol.* 1980;55(4):229–233.
26. Maia M, Kellner L, de Juan E Jr, et al. Effects of indocyanine green injection on the retinal surface and into the subretinal space in rabbits. *Retina.* 2004;24(1):80–91.
27. Lopez PF, Yan Q, Kohen L, et al. Retinal pigment epithelial wound healing in vivo. *Arch Ophthalmol.* 1995;113(11):1437–1446.
28. Roider J, Michaud NA, Flotte TJ, Birngruber R. Response of the retinal pigment epithelium to selective photocoagulation. *Arch Ophthalmol.* 1992;110(12):1786–1792.
29. Reh TA, Fischer AJ. Retinal stem cells. *Methods Enzymol.* 2006;419:52–73.
30. Fischer AJ, Reh TA. Potential of Muller glia to become neurogenic retinal progenitor cells. *Glia.* 2003;43(1):70–76.
31. Reh TA, Fischer AJ. Stem cells in the vertebrate retina. *Brain Behav Evol.* 2001;58(5):296–305.
32. Fischer AJ, Reh TA. Muller glia are a potential source of neural regeneration in the postnatal chicken retina. *Nat Neurosci.* 2001;4(3):247–252.
33. Tropepe V, Coles BL, Chiasson BJ, et al. Retinal stem cells in the adult mammalian eye. *Science.* 2000;287(5460):2032–2036.
34. Raymond PA, Hitchcock PF. How the neural retina regenerates. *Results Probl Cell Differ.* 2000;31:197–218.
35. Ahmad I, Tang L, Pham H. Identification of neural progenitors in the adult mammalian eye. *Biochem Biophys Res Commun.* 2000;270(2):517–521.
36. Raymond PA, Hitchcock PF. Retinal regeneration: common principles but a diversity of mechanisms. *Adv Neurol.* 1997;72:171–184.
37. Ooto S, Akagi T, Kageyama R, et al. Potential for neural regeneration after neurotoxic injury in the adult mammalian retina. *Proc Natl Acad Sci U S A.* 2004;101(37):13654–13659.